Terahertz Wave Detection Property of Polycrystalline GaAs Layer Irradiated by Ultra-short Laser Pulse

M. C. Paek[1], D. S. Jun[1], S. Y. Jeong[2], S. I. Kim[1], H. C. Ryu[1], M. H. Kwak[1], S. B. Kang[1], T. Y. Kim[1], and K. Y. Kang[1]

[1]Electronics and Telecommunications Research Institute, Terahertz Research Team, 138 Gajeong-ro, Yuseong-gu, Daejeon Korea

[2]School of Nanoscience and Technology, Chungnam National University, 99 Daehak-ro, Yuseong-gu, Daejeon Korea

***Abstract*- We have investigated the effects of crystal defects on detection of terahertz waves in a polycrystalline GaAs layer irradiated by ultra-short pulse laser. The poly-GaAs layer was grown by a molecular beam epitaxy(MBE) system at abnormally lower temperature of 150°C and *in-situ* annealed at 600°C. Lifetime and mobility of photo-generated charge carriers in the poly-GaAs layers were measured and compared with those of the normally grown epi-GaAs layers. Grain boundaries in the poly-GaAs layer and As precipitates in the epi-GaAs layers were both responsible for trapping of the charge carriers. Terahertz wave radiation detected with a photoconductive antenna device fabricated by using the poly-GaAs layer showed a higher signal to noise ratio than those of the epi-GaAs layers. Measurement and calculated results of mobility and terahertz wave detection properties revealed that the grain boundaries are more efficient than the As precipitates for the trapping of the photo-generated carriers..**

I. INTRODUCTION

Low temperature grown GaAs layers (LT-GaAs) containing As-precipitates are the most successfully employed material for a generation and detection of pulse and continuous THz waves for time domain spectroscopy and T-ray imaging.[1] Epitaxial LT-GaAs layers have long been used on account of its high mobility, high breakdown voltage and short carrier life-time[2-6]. It has been reported that micro-defects known as As-precipitates produced during the growth in As-rich environment play a role of trapping the photo-generated charge carriers[7,8]. So, the control of density and size of the As-precipitates is one of the important factors for the high quality terahertz wave. We have investigated instead a polycrystalline GaAs(poly-GaAs) layer grown at abnormally low temperature 150°C rather than epitaxial GaAs(epi-GaAs) layers grown at normal temperature 250~400°C. At the temperature lower than normal growth, poly-GaAs layers are grown instead of epi-GaAs layer after *in-situ* annealing[9,10]. For the terahertz application, the poly-GaAs layer has not been used so far because of the random nature of the grain boundaries and irregular shapes and orientation of the grains. Drawbacks of electrical and structural control of the polycrystalline layers containing grain boundaries have limited the usage of the poly-GaAs layers in the terahertz studies. However, carrier lifetime of the poly-GaAs layer is sufficiently short for the terahertz generation and detection [10]. In this work, we characterized the microdefects in the LT-GaAs layers and investigated the relationship with the mobility and lifetime of charge carriers photo-generated by ultra-short laser pulse.

II. EXPERIMENTS

2 inch diameter semi-insulating GaAs (SI-GaAs) wafers of (100) orientation were used as substrates for the growth of GaAs epitaxial layers. A conventional molecular beam epitaxy (MBE) system was employed to grow the GaAs layers. Temperature range of the growth was 150~400°C and growth time was fixed to 90min. In the MBE chamber, As-rich ambient has been maintained during the growth to produce point defects of As-precipitates which can play a role of trapping sites of photo-generated charge carriers generated by irradiation of ultra-short pulse laser beam. The As_4/Ga beam-equivalent-pressure (BEP) ratio in the chamber was 15~20. The grown GaAs layers were *in-situ* annealed in the MBE chamber at 600°C for 10min under an ambient of As overpressure. Microstructures of the GaAs layers were observed by using a high resolution transmission electron microscope and crystalline properties were characterized by x-ray rocking curve analysis. Carrier lifetime of the photo-generated electrical charges and electrical mobility of the carriers were measured by using a time resolved reflectivity spectrometry and a Hall measurement system, respectively.

The properties of generation and detection of terahertz waves were measured by irradiation of ultra-short laser pulses into photoconductive antenna devices patterned on the LT-GaAs layers. The terahertz photoconductive antenna (PCA) devices were fabricated by depositing Ti/Au contact metal on the surface of the LT-GaAs layers and patterning it with a standard lift-off process. A dipole antenna of 10μm width and 5μm center gap was patterned for the detection, and a coplanar transmission line of 10μm width and 29μm separation for the generation of the terahertz waves. DC bias voltage at the photoconductive antenna was 20V. A high resistivity hyper-hemispherical silicon lens was attached to the backside of the SI-GaAs substrate of the antenna device in order to reduce the reflection loss at the air-substrate interface and to enhance the radiation collection efficiency. The terahertz wave experiments have been carried out by using a conventional terahertz time domain spectroscopy (THz-TDS) system. The excitation source was a mode-locked Ti: sapphire (Al_2O_3) laser with a pulse width ≈30fs and a repetition rate 80MHz. The center wavelength of the laser was 794.4 nm. The photoconductive antenna device with a 350°C grown LT-GaAs layer was used for the generation of terahertz waves, and the detection properties of 150, 250, 300 and 400°C grown GaAs layers

were measured. The incidence laser powers on generation and detection devices were 10 and 15mW, respectively. And the THz-TDS system was enclosed in a N_2-purged dry station to reduce the terahertz wave power absorption due to residual water vapors in the air of the terahertz wave beam path. Fig. 1 shows a configuration of the THz-TDS system used for the detection of terahertz waves.

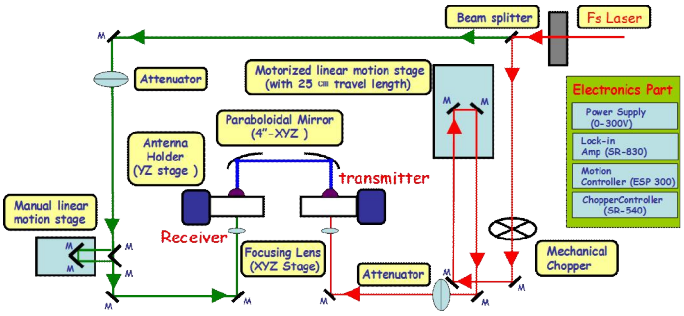

Fig. 1 Configuration of THz-TDS system used for the measurement of the terahertz detection properties of the LT-GaAs layers

III. Results & Discussion

Cross section transmission electron micrographs of the LT-GaAs layers are shown in Fig. 2. In the as-grown state of the layer grown at 150°C, the image contrast owing to dislocation loops and extended dislocations are clearly seen inside the layer, while in that grown at 250°C, any image contrast due to crystal defects are not observed. The distribution of the dislocation loops through the thickness of the layer grown at 150°C. After 600°C *in-situ* annealing, the dislocation-containing layer has recrystallized to a polycrystalline state. The transmission electron micrograph with a corresponding electron diffraction pattern of the layer points out that epitaxial growth of the layer have already been destroyed at the initial growth stage, and the orientation and size of the grains are randomly distributed through the thickness of the layer, revealing that the stress produced by the excess As atoms have existed during the growth and annihilated by producing crystal defects. The high resolution image of the layer-substrate interface illustrates that there is no more crystalline coherency between the SI GaAs substrate and the poly-GaAs layer. And any evidence of the As-precipitates are not found in the image, suggesting that during the annealing process, excess As atoms move to the grain boundaries and agglomerate at the inter-grain sites or diffuse out to the surface through the grain boundary channel. The range of grain size of the poly-GaAs layer was measured to be 50 ~ 300nm and average grain size was 210nm diameters. Microanalysis of the As concentration at the grain boundaries using an energy dispersive x-ray spectrometry (EDX) informed that there was not a big difference of atomic concentration of As between inter and intra granular position within the detection limit of EDX system (0.1~1.0 atomic %). As a consequence, it seems that most of the excess As atoms have escaped out of the layer by diffusion during the annealing process. The cross section morphologies of the layers grown at 250 to 400°C and *in-situ* annealed at 600°C respectively, indicate that the layers are single crystalline with corresponding electron diffraction patterns showing typical [2-20] spot patterns. In the layers, uniformly distributed black dots are observed, and the size and the dot-to-dot space distance are 2~30nm. The high resolution images of the layers point out that the dots are As precipitates produced during the *in-situ* annealing. Youn et. al.[8] have characterized the dots to be As precipitates by using EDX microanalysis and high resolution lattice images of Moire fringe caused by overlapping the crystallites of As_4 precipitates with the GaAs matrix. Average size and density of the precipitates more or less depend on the growth temperature of the layer. The diameter of the precipitates increases and the density decreases with the growth temperature as noted in Table 1. Most of the excess As atoms have escaped out of the layer during the followed heat treatment at 600°C and the amount of the residual As atoms in the layer influence the distribution behavior of the As precipitates after *in-situ* annealing.

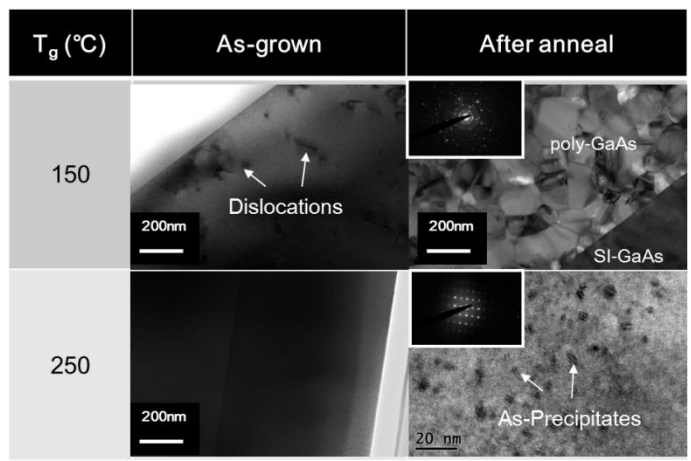

Fig. 2 Cross section transmission electron micrographs for LT-GaAs layers of as-grown and after *in-situ* annealing showing poly- and epi GaAs states

Fig. 3 shows high resolution x-ray diffraction double crystal rocking curves (DCRC) of GaAs (400) peak for the LT-GaAs layers grown at various temperatures. The GaAs (400) peak at θ=33.023° is due to the SI-GaAs substrates and the side peak at left shoulders are associated with the LT-grown GaAs layers. The curves of the layers grown at 250, 300 and 400°C show that additional side peaks are observed at the slightly small diffraction angle from the (400) peak in as-grown states and then disappear after 600°C *in-situ* annealing. During the growth of the GaAs layers at low temperature in an As-rich ambient, the excess As atoms are incorporated in the layer, because the excess As atoms do not have sufficient energy to escape out of the layers. Thus, at the lower growth temperature, the number of the incorporated excess As atoms must be higher. The peaks observed at the left side of the GaAs (400) peak indicate that excess As atoms positioned in the interstitial and anti-site cause the compressive strain in the GaAs lattice and then increase the lattice parameter and make the crystalline properties unstable. The separation distance between side peaks and (400) peak increase with decreasing growth

temperature. The expansion of the lattice parameters can be calculated by using Bragg's law,

$$\frac{\Delta d}{d} = \frac{\Delta\theta}{\theta} \qquad (1)$$

where, d and Δd the lattice parameter and the increment, and θ and $\Delta\theta$ the diffraction angle and the increment. In this work, the increase of lattice parameters during the growth of the LT-GaAs layers were calculated to be 0.130, 0.094 and 0.036% at the growth temperature of 250, 300 and 400°C, respectively. On the other hand, poly-GaAs layer grown at 150°C shows only (400) GaAs peak, and the side peaks are not observed. It suggests that 150°C is not an enough temperature for the epitaxial growth of the layer, and the compressive strain due to the excess As atoms is too high to maintain the epitaxial crystallinity of the layer. Thus, to release the stress in the layers, crystal defects such as dislocations, stacking faults and anti-phase boundaries have to be produced in the layer, and therefore the change of lattice parameter and additional side peak are not observed in the x-ray rocking curve. After 600°C *in-situ* annealing, the side peaks are not observed for all of the GaAs layers any more. It indicates that the excess As atoms in the off-lattice sites have redistributed and agglomerated to generate As-precipitates in a stable crystalline state with sufficient thermal energy.

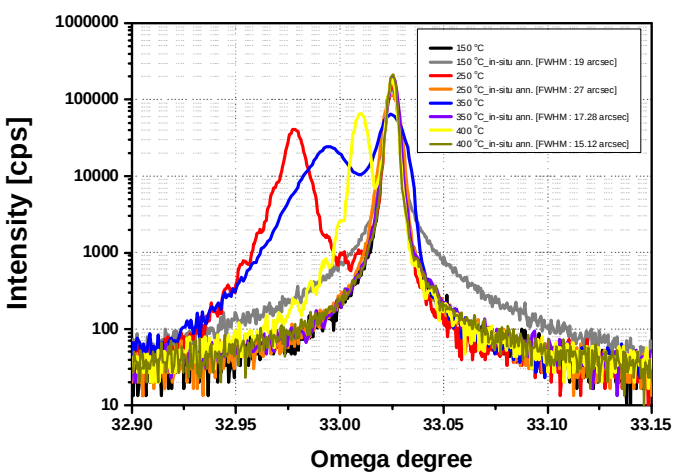

Fig. 3 X-ray rocking curves of LT-GaAs layers for as-grown at various temperatures and *in-situ* annealed.

The As precipitates in LT-GaAs normally take a role of the recombination center for charge carriers which have been generated by ultra-short laser pulse irradiation. For high signal to noise ratio of terahertz waves, a high mobility and a short carrier lifetime are necessary conditions of the GaAs layers, and intentionally formed As precipitates can shorten the carrier lifetime. Fig. 4 shows the carrier lifetime of the LT-GaAs layers according to the growth temperature measured by time resolved reflection spectrometry. The poly-GaAs layer grown at 150°C shows the shortest carrier lifetime and for those of the epi-GaAs layers the lifetime increase with the growth temperature, indicating that the microstructure and the distribution of crystal defects are closely related to the behavior of the charge carriers. Grain boundaries and As precipitates are strong capturing sites of the carriers. The grain boundaries have higher energy states than the inside of the grain, and there exist a lot of dangling bonds and interface state charge. Thus, transient level energy states could be generated in the band gap of GaAs, and then they will work as recombination centers for electron-hole pairs.

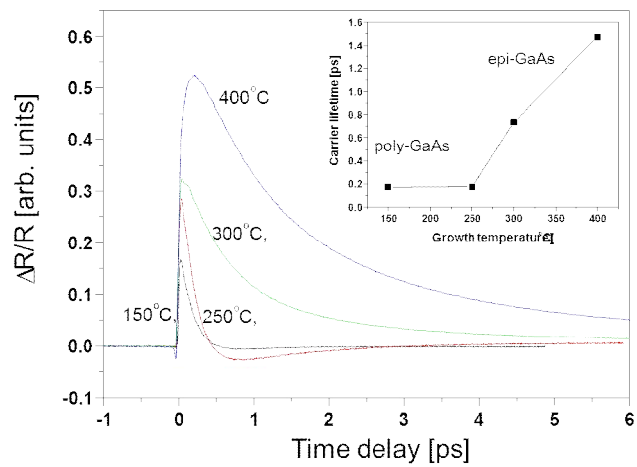

Fig. 4 Carrier lifetimes of the poly-GaAs and epi-GaAs layers grown at various temperatures and *in-situ* annealed at 600°C.

Fig. 5 shows measurement results of the mobility and carrier density of the GaAs layers by using a Hall measurement and a van der Paw method. In Fig. 5, the poly GaAs shows the higher electrical mobility and the lower carrier density than those of the epi-GaAs layers. The mobility of the charge carriers in the LT-GaAs layers must be strongly influenced by the behavior of the micro-defects. We have calculated the mobility of the charge carriers by considering a simple model.

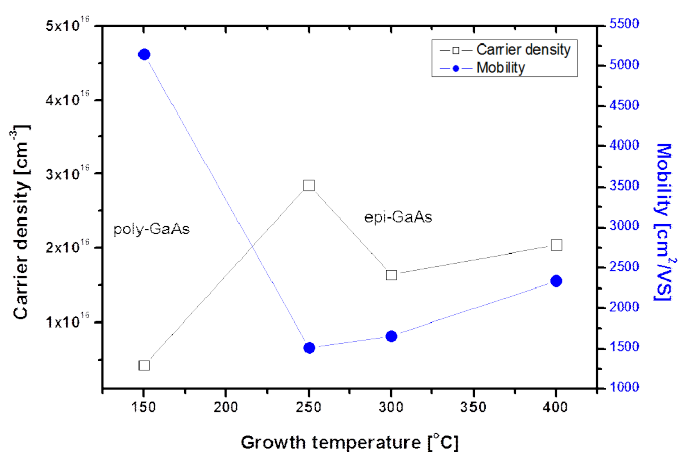

Fig. 5 Mobility and carrier density of the poly-GaAs and epi-GaAs layers grown at various temperatures and *in-situ* annealed at 600°C.

Mobility of the electrical carriers is generally denoted by,

— (2)

where μ_{dc} is the usual mobility of the material, and v_d the drift velocity and E the electric field due to DC bias voltage on the photoconductive antenna. The average drift velocity can be obtained by dividing the travel distance by the carrier lifetime. The travelling distance of the photo-generated charge carriers in the poly-GaAs layer could be the same as the average diameter of the grains. So, the average drift velocity of the electrical charge carriers in poly-GaAs layer is 1.21×10^8cm/s. When we consider the DC bias voltage 20V and 5μm center gap, the dc mobility is calculated to be 3,017cm^2/V.s.

In the epi-GaAs layers containing As precipitates, the travelling distance of the charge carriers have to be determined by another way. Here we have imported the concept of a mean free path. By assuming that the mobile particles (electrons and holes in this work) have a Maxwell distribution of velocities, the mean free path of the carriers through the As precipitates can be given by[11]

– (3)

where l the mean free path of the charge carriers, σ the scattering cross section of the collision particles (As precipitates), and n the number of particles in unit volume (density of the As precipitates). σ can be given by the average cross sectional area of the As precipitates,

– (4)

where d the average diameter of As precipitates. The density of the As precipitates in the layer n can be calculated by assuming that the As precipitates are uniformly distributed at the position of diamond cubic lattice points with a constant space s, and then it can be given by

. (5)

The mean free path of the mobile particles in the layer, the travelling distance of the charge carriers l, in eq (3) can be given by using eq. (4) and (5)

Table 1 denotes a relationship of lifetime and dc mobility to the travel distance of the carriers determined by transmission electron micrographs and eq. (6). The calculated values of mobility in Table 1 and the measured ones in Fig. 4 have a same trend of increase at temperature region where the GaAs layers have grown epitaxially. It shows that the introduction of the mean free path and the assumptions for the calculations are consistent with the real process. The poly-GaAs layer grown at 150°C shows the highest value of the mobility both for measured and calculated results. It means that the carriers move more rapidly in the each grains of the polycrystalline than in the epitaxial matrix containing As precipitates. The carrier density of the poly-GaAs layer in the Fig.4, however, shows the lowest value, indicating that the grain boundaries are stronger trapping sites of the charge carriers.

(6)

Table 1 Calculation of carrier mobility in the LT-GaAs layers

Tg. (°C)	*150*	*250*	*300*	*400*
Crystal structure	Poly *l*=210nm	Single d=2.5nm s=7.4nm	Single d=2.7nm s=12.4nm	Single d=5.2nm s=28.4nm
Travel distance (nm)	210	89.9	362.8	1,175.0
Lifetime τ (ps)	0.174	0.194	0.738	1.47
mobility μ_{dc} (cm^2/V.s)	3,017	1,177	1,228	1,998

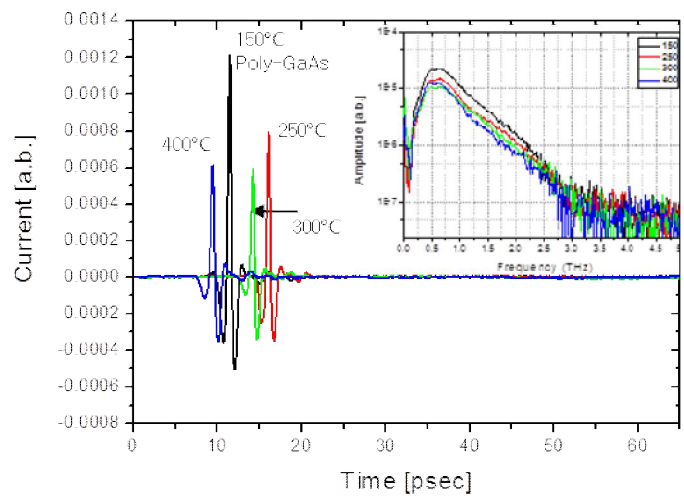

Fig. 6 Measured terahertz wave forms and frequency domain spectra inset for the LT-GaAs layers grown at various temperatures

Terahertz waves detected by a typical photoconductive antenna based terahertz time domain spectroscopy (THz-TDS) system are shown in Fig. 6 for the GaAs layers grown at 150, 250, 300 and 450°C, and annealed at 600°C, respectively. Inset in the graph are the corresponding frequency domain spectra of the terahertz waves. For all of the GaAs layers, the bandwidths of the terahertz wave are in the range of 0.1 to 3.0THz. The signal to ratio of terahertz wave detected with the poly-GaAs layer is higher than those with the epi-GaAs layers. For the single crystalline layers containing As precipitates, dependence of the signal to ratio on the growth temperature is not so strong. It is consistent with the variation of the mobility values measured and calculated as shown in Fig. 5 and Table 1.

IV. Conclusion

We have investigated a relationship between microstructure of the defects and terahertz wave detection property in the LT GaAs layers. The grain boundaries in the poly-GaAs layer grown at abnormally lower temperature and the As precipitates

in the epi-GaAs layers both responsible for the trapping of photo-generated charge carriers by irradiation of ultra-short pulse laser. The poly-GaAs layer showed the shortest carrier lifetime and the highest mobility. Grain boundary effects and a mean free path were employed to calculate the mobility in the poly- and epi-GaAs layers. The calculated values show a consistency with the measured ones, indicating that the assumptions and the concept of mean free path have validity. The highest signal to noise ratio of terahertz wave detection was obtained with the poly-GaAs layers, pointing out that the poly-GaAs layer can be used in the photoconductive emission and detection of terahertz waves. Poly-GaAs layers can be grown on any substrates other than SI GaAs such as silicon, quartz, sapphire etc. It opens the possibility of changing the substrate and growing methods to realize high efficiency photoconductive devices with low processing costs for the terahertz wave systems.

REFERENCES

[1] H.B. Liu, H. Zhong, N. Karpowicz, Y. Chen, and X.-C. Zhang, "Terahertz spectroscopy and imaging for defence and security applications," *Proc. IEEE*, vol. 95, no. 8, pp. 1514–1527, Aug. 2007

[2] D. H. Auston, K. P. Cheung, and P. R. Smith, "Picosecond photo-conducting Hertian dipoles", Appl. PHys. Lett., 45(3) pp. 284-286 (1984)

[3] A. C. Warren, N. Katzenellenbogen, D. Grischkowsky, J. M. Woodall, M. R. Melloch, and N. Otsuka, "Subpicosecond, freely propagating electro-magnetic pulse generation and detection using GaAs:As epilayers", Appl. Phys. Lett., 58(14) pp.1512-1514 (1991)

[4] M .B. Ketchen, D. Grischkowsky, T. C. Chen, C-C. Chi, I. N. Durling, III, N. J. Halas, J-M. Halbout, J. A. Kash, and G. P. Li, "Generation of sub-picosecond electrical pulses on coplanar transmission lines", Appl. Phys. Lett., 48(12) pp.751-753 (1986)

[5] Y. C. Shen, P. C. Upadhya, E. H. Linfield, and H. E. Beere, "Ultrabroadband terahertz radiation from low-temperature-grown GaAs photoconductive emitters", Appl. Phys. Lett., 83(15) pp.3117-3119 (2003)

[6] Y. C. Shen, P. C. Upadhya, H. E. Beere, E. H. Linfield, A. G. Davies. I. S. Gregory, C. Baker, W. R. Tribe, and M. J. Evans, "Generation and detection of ultrabroadband terahertz radiation using photoconductive emitters and receivers", Appl. Phys. Lett., 85(2) pp.164-166 (2004)

[7] M. Fatemi, B. Tadayon, M. E. Twigg, and H. B. Dietrich, "High-temperature x-ray analysis of strain in low-temperature GaAs", Phy. Rev. B, 48(12), pp.8911-8917 (1993)

[8] D. H. Youn, S. H. Lee, H. C. Ryu, S. Y. Jeong, S. B. Kang, M. H. Kwak, S. I. Kim, S. K. Choi, M. C. Baek, K. Y. Kang, C. S. Kim. K. J. Yee, Y. B. Ji, E. S. Lee, T. I. Jeon, S. J. Kim, S. Kumar, and G. H. Kim, "Effects of post-growth annealing on the structure and electro-optical properties of low-temperature grown GaAs", J. Appl. Phys. 103, 123528 (2008)

[9] J. J. J. Yang, P. D. Dapkus, R. D. Dupuis, and R. D. Yingling, "Electrical properties of polycrystalline GaAs films", J. Appl. Phys. 51(7) pp3794-3800 (1980)

[10] J-F. Roux and J-L Coutaz, "Time-resolved reflectivity characterization of polycrystalline low-temperature-grown GaAs", Appl. Phys. Lett., 74(17) pp.2462-2464 (1999)

[11] Se Young Jeong, et al., "Terahertz Detection with Polycrystalline GaAs Films",*Tera Tech 09 (2nd International Workshop on THz Technology, Osaka Japan* 1P-06, 2009